Wind and Structures, Vol. 14, No. 5 (2011) 383-411
DOI: http://dx.doi.org/10.12989/was.2011.14.5.383

Generalized load cycles for dynamic wind uplift evaluation of rigid membrane roofing systems

Baskaran, A.*[1], Murty, B.[2] and Tanaka, H.[2]

[1]*National Research Council of Canada, 1200 Montreal Rd., Ottawa, Canada, K1A 0R6*
[2]*Department of Civil Engineering, University of Ottawa, Ottawa, Canada, K1N 6N5*

(Received March 9, 2010, Accepted January 11, 2011)

Abstract. Roof is an integral part of building envelope. It protects occupants from environmental forces such as wind, rain, snow and others. Among those environmental forces, wind is a major factor that can cause structural roof damages. Roof due to wind actions can exhibit either flexible or rigid system responses. At present, a dynamic test procedure available is CSA A123.21-04 for the wind uplift resistance evaluation of *flexible* membrane-roofing systems and there is no dynamic test procedure available in North America for wind uplift resistance evaluation of *rigid* membrane-roofing system. In order to incorporate rigid membrane-roofing systems into the CSA A123.21-04 testing procedure, this paper presents the development of a load cycle. For this process, the present study compared the wind performance of rigid systems with the flexible systems. Analysis of the pressure time histories data using probability distribution function and power spectral density verified that these two roofs types exhibit different system responses under wind forces. Rain flow counting method was applied on the wind tunnel time histories data. Calculated wind load cycles were compared with the existing load cycle of CSA A123.21-04. With the input from the roof manufacturers and roofing associations, the developed load cycles had been generalized and extended to evaluate the ultimate wind uplift resistance capacity of rigid roofs. This new knowledge is integrated into the new edition of CSA A123.21-10 so that the standard can be used to evaluate wind uplift resistance capacity of membrane roofing systems.

Keywords: wind uplift; rigid roof; flexible roof; dynamic procedure; wind tunnel; design pressure; certification.

1. Introduction

Roof is an integral part of the building envelope that protects occupants from the environmental forces such as wind, rain, snow, temperature gradients, solar radiation, etc. Among those environmental forces, wind can cause major structural damages to roofing systems (Baskaran 1986, Smith 2009). Understanding roofs performance under wind actions is important to quantify its wind uplift performances. Roofs can be classified as either low-slope or steep-slope. Low-slope roofs are often installed in commercial and industrial buildings such as warehouses and factories, while residential buildings mostly have steep-slope roofs. In terms of its response due wind actions, low slope roofs can exhibit either rigid or flexible responses. The roof response depends on the types of attachment used for the roof components. Further information about the common types of low-slope

* Corresponding Author, Dr., E-mail: bas.baskaran@nrc.ca

roof attachments and components can be found in Laaly (1992). Fig. 1 shows typical examples of rigid and flexible membrane-roofing systems. Rigid roof is a type of roof in which all components unite together and share the wind uplift forces (Phonemic load transfer mechanism), while for the flexible roofs, most of membrane tensions are transferred to the structural deck through fasteners (Linear load path mechanism). Fig. 2 describes the two roof system responses under wind actions as well as their force dissipation diagrams.

A dynamic testing procedure available in the North America is “CSA A123.21-04 entitled

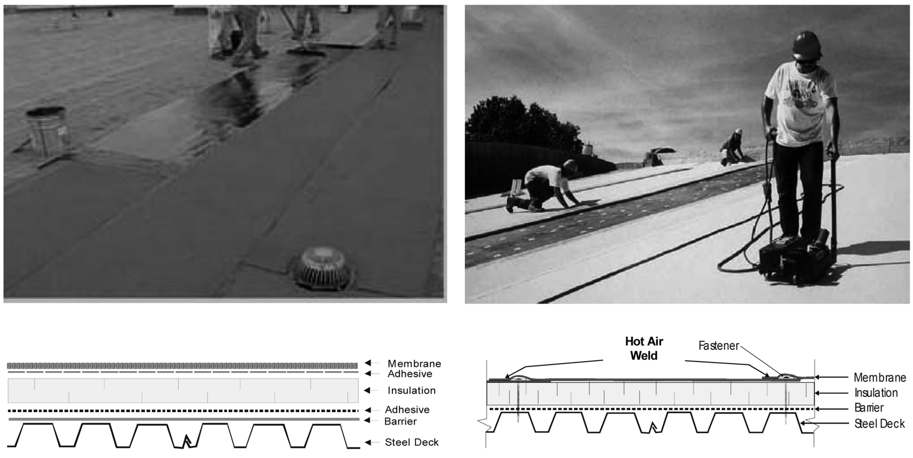

Typical rigid roofing system

Typical flexible roofing system

Fig. 1. Typical examples of rigid and flexible roofing systems

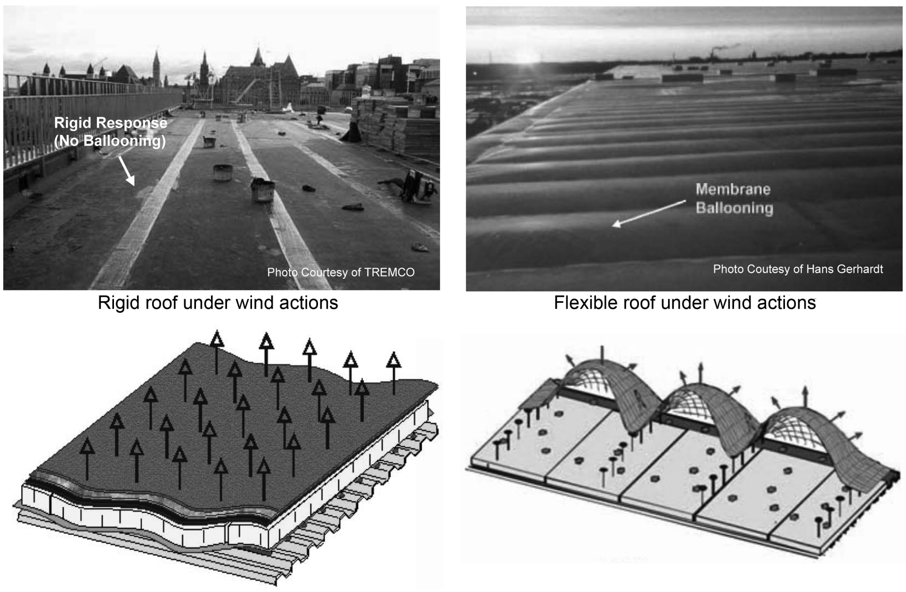

Rigid roof force dissipation diagram

Rigid roof force dissipation diagram

Fig. 2 Roof system responses and force dissipation diagrams

Standard Test Method for the Dynamic Wind Uplift Resistance of Mechanically Attached Membrane-Roofing Systems". The "CSA A123.21-04" was specifically developed to evaluate wind uplift performance of mechanically attached flexible membrane roofing systems. There is no dynamic test procedure available to evaluate wind uplift performance of rigid membrane-roofing systems (Murty 2009). In order to incorporate rigid membrane-roofing systems into the CSA A123.21-04 testing procedure, this paper presents the development of a load cycle. For this process, the present study compares the wind performance of rigid systems with the flexible systems. Analysis of the pressure time histories data using probability distribution function and power spectral density verify that these two roofs types exhibit different system responses under wind forces. The load cycle for the evaluation of rigid roofing system is developed using wind tunnel data by applying rain flow counting method. Calculated wind load cycles are compared with the existing load cycle of CSA A123.21-04. With the input from the roof manufactures and roofing associations, the developed load cycles has been generalized and extended to evaluate the ultimate wind uplift resistance capacity of rigid roofs. This new knowledge is in the process of integrating into the new edition of CSA A123.21 so that the standard can be used to evaluate wind uplift resistance capacity of membrane roofing systems.

2. Wind tunnel data on models with flexible roofs

A Special Interest Group for Dynamic Evaluation of Roofing Systems (SIGDERS) was formed in 1994 by the National Research Council Canada (NRCC) and its members include the roofing contractors' associations, manufacturers and building owners / managers. The research activities initiated by SIGDERS have made a significant contribution to the North American roofing community. Among them is the development of the dynamic testing procedures for the evaluation of the wind uplift performance of mechanically attached flexible membrane roofing systems (CSA A123.21-04). The SIGDERS load cycle was developed based on wind tunnel studies using a full scale model of the flexible membrane roofing systems (3 m by 3 m). Wind tunnel experiments were carried out at the NRCC's 9 m by 9 m wind tunnel. Further details of the wind simulation data and tested configurations are available elsewhere (Savage *et al.* 1996, Baskaran *et al.* 1996, Baskaran *et al.* 1997, Chen and Baskaran 1997, Baskaran *et al*. 1999). Seventy eight flexible roof configurations using two types of roof membrane, *PVC (Poly Vinyl Chloride) and EPDM (Ethylene Propylene Diene Monomer)*, were tested. Fig. 3 shows typical pressure coefficient contour plots from the two types of flexible membrane used during SIGDERS wind tunnel test. Pressure taps were installed on the roof assemblies and the data collected from the pressure taps were analyzed by the rain flow counting (RFC) method. The performed data analysis resulted in establishment of the SIGDERS load cycles as shown in Fig. 4 and later the load cycle has been adopted by the CSA A123.21-04 as load testing protocol to evaluate mechanical attached flexible membrane roofing systems.

As shown in Fig. 4, the CSA dynamic protocol has five rating levels (A to E). To evaluate a roof assembly for a specific wind resistance, all the gusts corresponding to Level A should be applied. Each level consists of eight load sequences with different pressure ranges. The eight load sequences are divided into two groups. Group 1 represents wind-induced suction over a roof assembly. It consists of four sequences, where the pressure level alternates between zero and a fixed pressure. Group 2 represents the effects of exterior wind fluctuations combined with a constant interior pressure on a building. Internal pressure variations are explicitly codified in the recent North

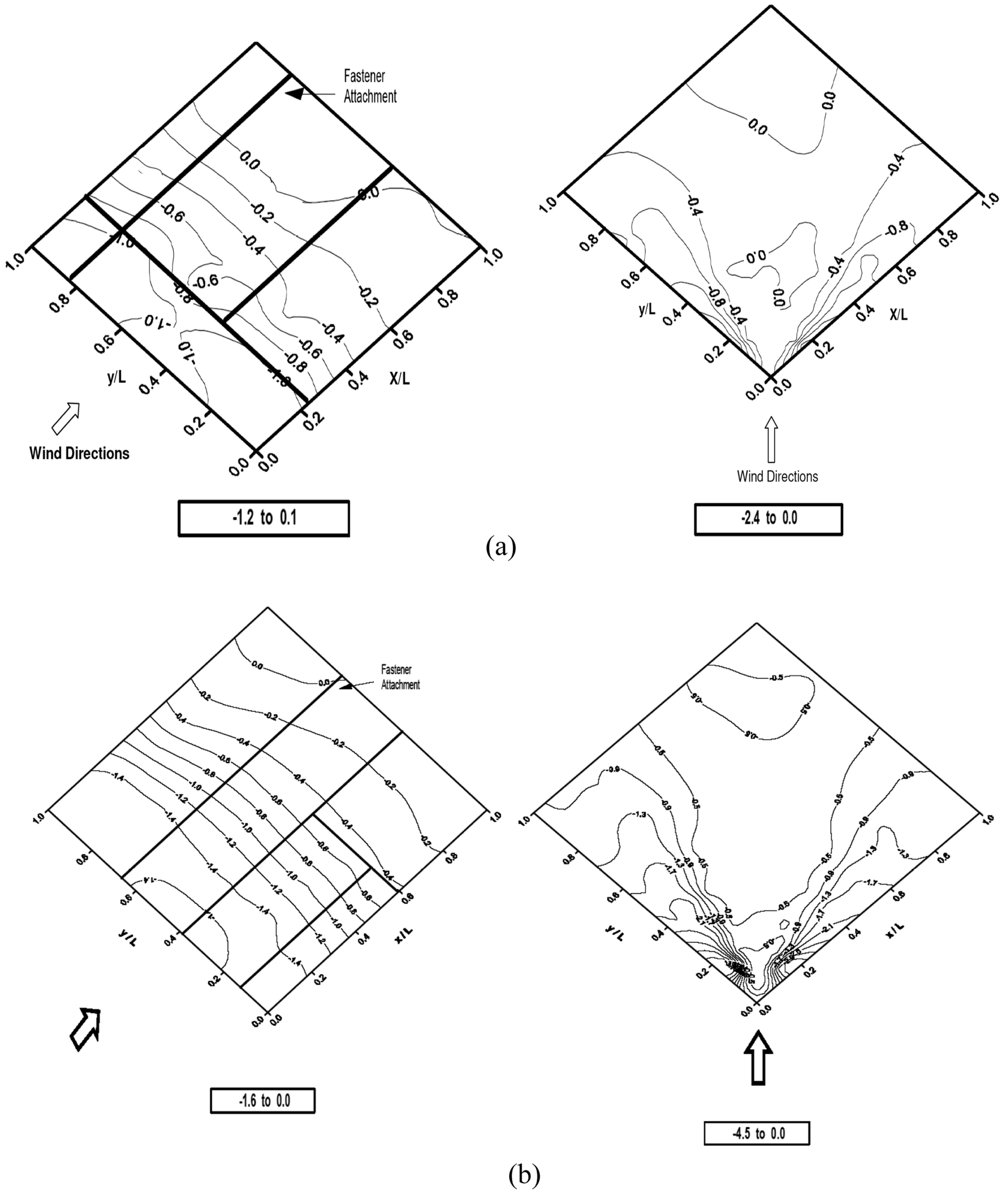

Fig. 3 (a) Pressure coefficient contour plot for PVC and (b) pressure coefficient contour plot for EPDM

American wind standards (ASCE 7-2005, NBCC 2005). The CSA test protocol accounts for such variations (Baskaran *et al*. 1999). The test pressure ratios (y-axis), P, 1.25P, 1.5P, etc, can be calculated from the design pressure, in accordance with local building codes or wind standards. The pressures for each load sequence are calculated as percentages of the test pressure (P). To evaluate the ultimate strength of the roofing assembly, testing should be started at Level A and should be continued when moving from one level to another. To obtain a rating, all specified numbers of gusts in each level must be completed without any resistance link failure.

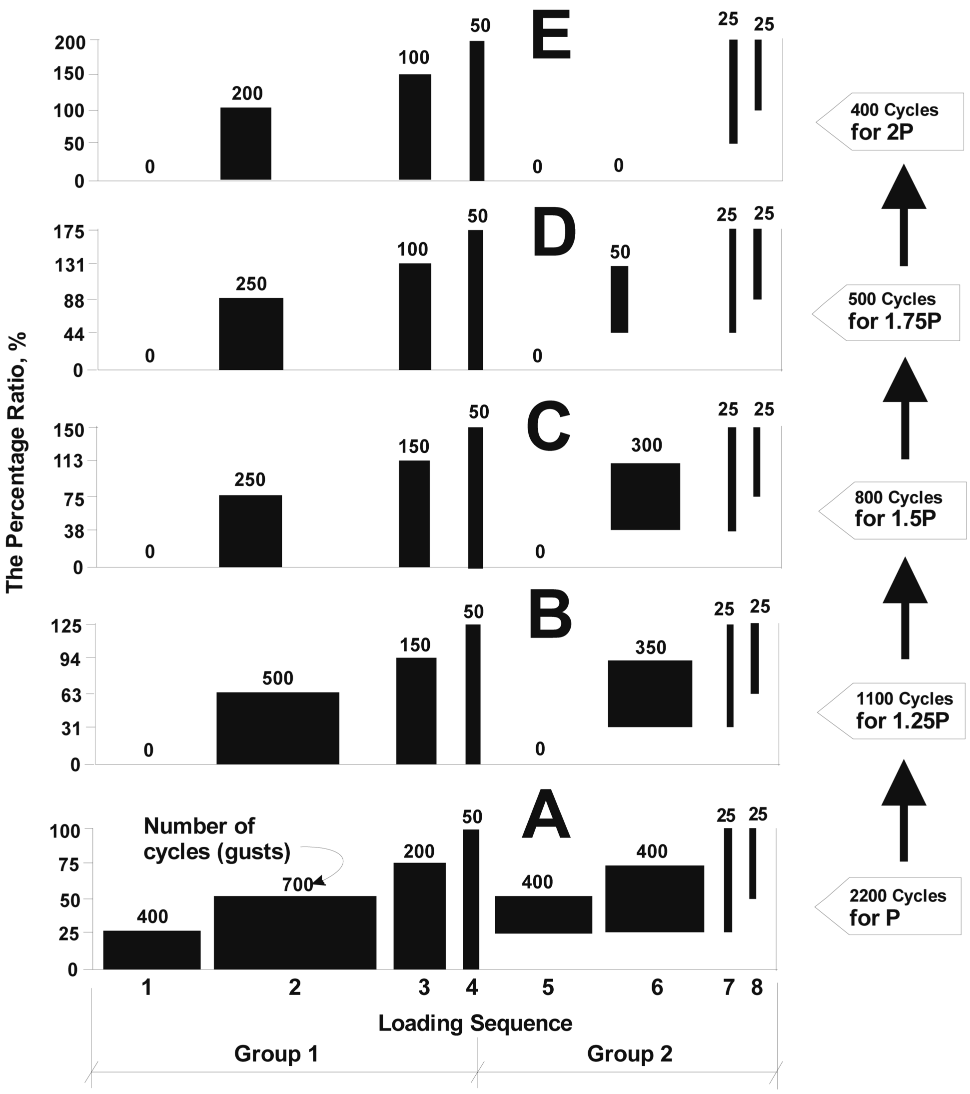

Fig. 4 Load cycle for wind uplift resistance evaluation of flexible roofing systems (CSA A123.21-04)

2.1 Wind tunnel data on models with rigid roofs

The results from the wind tunnel test carried out at the Concordia University by Stathopoulos (2008), were used by the present study. The wind tunnel roof model was rigid and tested under open exposure condition for three different building heights, three different building aspect ratios and two different wind angles (Table 1). The time histories of measured pressure data obtained from the tests were converted into dimensionless pressure coefficients (Cp) referenced to the building roof height. During the wind tunnel testing, the pressure time histories were collected using a sampling frequency of 418.75 Hz over a period of 64 seconds, resulting in 26800 data points for each pressure tap. The test conditions and configurations presented in Table 1 were specifically

Table 1 Test condition and configuration used for the wind tunnel study with rigid roof

Parameter	Description
Test condition	Open exposure
Height (ft/m)	20/6.1, 40/12.2 and 60/18.3
Roof aspect ratio	0.5, 1 and 2
Roof / Building Size (ft/m^2)	(20/6.1 x 20/6.1), (20/6.1 x 40/12.2), and (40/12.2 x 20/6.1)
Wind angle (degrees)	0 and 45
Number of pressure taps	15

designed so that at later stage these data can be compared with the previously collected data on flexible roofs. The open exposure was selected to be conservative; the selected three different heights cover the different heights within the category of low-rise buildings. Three aspect ratios represent common building shapes conceivable for low slope application. The two wind angles were selected to consider differences between two extreme cases. Fig. 5(a) shows the wind tunnel model with a rigid roof. Data from the locations of 15 pressure taps were selected in such a way that the collected data can be compared with the SIGDERS wind tunnel data to examine the difference of the wind effects between rigid and flexible roofs. Fig. 5(b) indicates the locations of the 15 pressure taps that are presented in terms of the ratio to either building width (W) or building length (L). The intention was to provide general data that do not depend on the building width or length. Thus, the data collected can be compared to any wind tunnel data that has a similar set-up to the rigid roof models tested. Regardless of the efforts made, it is noticed that the number of pressure taps used in the current model was less than the flexible model. The pressure taps location might affect the measurement of worst suction on roof. However, the present research is focused on the number of occurrences for a typical suction on a roof zone. Thus, why, for the purpose of data analysis, the pressure tap locations were divided into three roof zones, namely, corner (C), perimeter (S) and field (r) as illustrated in Fig. 5(b). This approach provided direct comparison between rigid and flexible roofs.

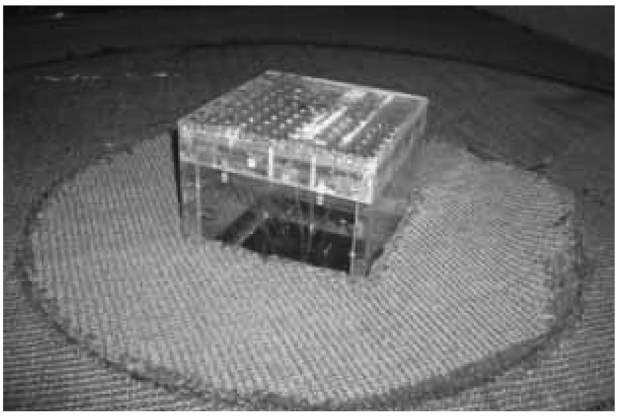

(a) Typical wind tunnel model with rigid roof, aspect ratio = 1, H/W = 1

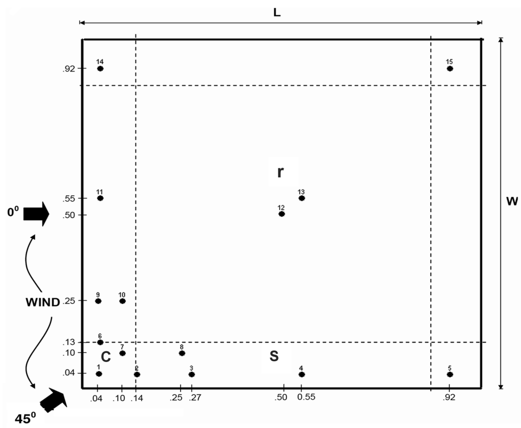

(b) Pressure tap locations on the wind tunnel model with rigid roof

Fig. 5 Typical wind tunnel model and pressure tap locations for rigid roof

2.2 Response of the wind tunnel model with rigid roof

In total, 270 time histories of measured pressure coefficients were obtained from the wind tunnel tests using rigid models for all test configurations and conditions as shown in Table 1. Fig. 6 illustrates a typical time history of the measured pressure coefficient. The graphs in Fig. 6 provide typical examples of the measured pressure coefficients time histories at three different heights. The data presented at each graph was collected from the same tap location (corner), roof aspect ratio (1) and wind direction (45^0). The horizontal axis illustrates the time in seconds while the vertical axis gives the dimensionless pressure coefficients. From the time histories, mean, root-mean-square (rms) and peak values of the measured suction coefficient (Cp) were calculated. Fig. 6 indicates that the

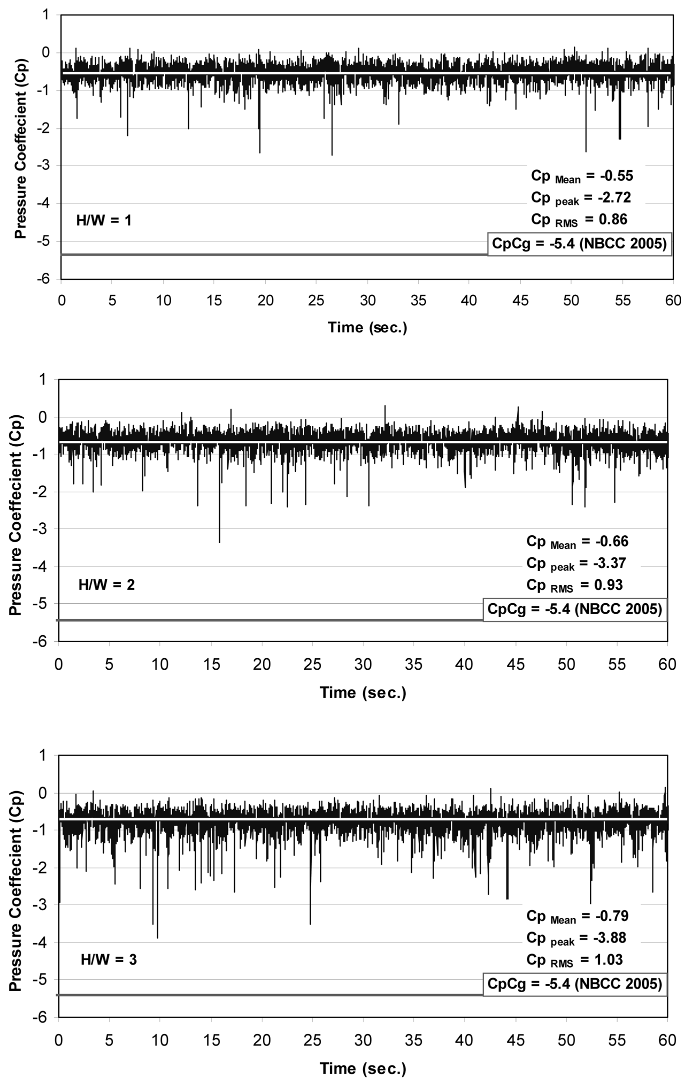

Fig. 6 Typical suction coefficient fluctuations for a corner pressure tap (roof aspect ratio = 1, wind direction = 45 degrees)

values of peak suction coefficient (Cp_{peak}) were influenced by the building height. It also can be seen from the Fig. that for the ratio of building height over width of the building (H/W) of 3 has the largest value of Cp_{peak} in comparison with the H/W ratio of 2 and of 1. The Cp_{peak} from the wind tunnel test can directly be compared to CpCg value obtained from NBCC (2005). This is because of gust effect and aerodynamic shape factor have been incorporated during wind tunnel testing (Clause 20-structural commentary I, wind load and effects, NBCC, 2005). Regardless of the building height that is presented in terms of H/W ratios, the value of Cp_{peak} was found to be lower than the value of CpCg given in the National Building Code of Canada (NBCC, 2005). This indicates that the code value is conservative. Fig. 7 shows the Cp_{peak} obtained from the pressure taps for the three roof zones, namely, Corner (C), Perimeter (S) and Field (r). This indicates that the Cp_{peak} vary across the roof surface. It was observed that the Cp_{peak} value was higher at the corner compared to other roof zones. This is because of vortices formed during wind flow on roofs. For the case of 0^0 approaching wind angle, the worst pressure is known to occur beneath the vortices that form in separated flow along the roof edge, while for the case of 45^0, it is caused by the dual conical vortices during cornering winds. Similar conditions were also observed on the other wind tunnel test investigations conducted by researchers such as Lawson (1980), Simiu and Scanlan (1986), Chen and Baskaran (1997), Baskaran *et al*.(1997), Uematsu *et al* (1999), Stathopoulos *et al* (1999) and Bank *et al* (2000). Fig. 7 also clearly shows that the wind direction influences the Cp_{peak} values. For the perimeter zone, it is noticed that the CpCg value predicted based on NBCC (2005) is some time lower than the Cp_{peak} values obtained from the wind tunnel test. Actually, this could happen due to the vortex wind flows on roof. Nevertheless, the observed Cp_{peak} values from the wind tunnel tests were found to be lower than the corner CpCg value of NBCC (2005). In addition to examining the effects of building height and wind direction, investigation was also extended to the influence of roof aspect ratio to the Cp_{peak} values and its distribution at various roof zones. Fig. 8 illustrates the Cp_{peak} values with the three roof aspect ratios considered across the three roof zones. The Cp_{peak} values presented in the Fig. 8 are the worst Cp_{peak} value from the two wind directions considered under the same roof aspect ratio, roof zone and building height. For example, the Cp_{peak} value of -4.46 for the aspect ratio of 1/2 at the corner location was the maximum measured Cp_{peak} value, when the model was tested at 0 to 45 degrees. Similarly, the other Cp_{peak} values for the three roof zones and roof aspect ratios were determined. Fig. 8 describes the Cp_{peak} values at the corner roof zone are always higher than at the perimeter or the field zones for any roof aspect ratios. It also shows that the roof aspect ratio influences the Cp_{peak} values under the same H/W ratio.

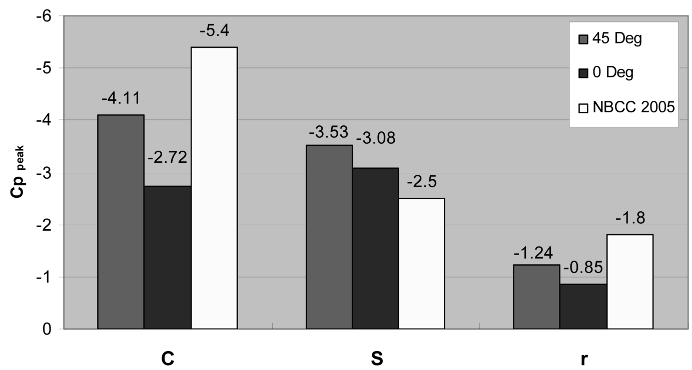

Fig. 7 Peak suction coefficients with different wind angles (H/W = 1)

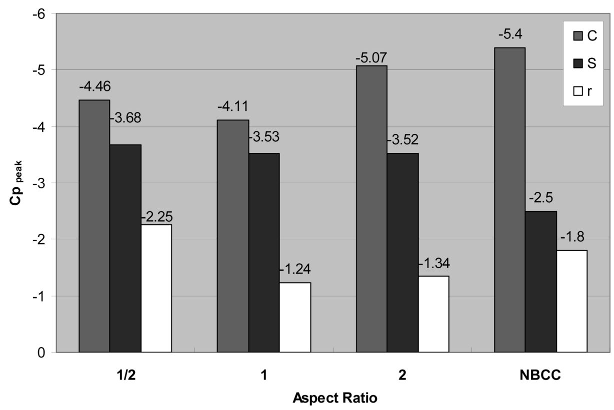

Fig. 8 Worst peak suction coefficients with different aspect ratios (H/W = 1)

Regardless any roof aspect ratios, the Cp_{peak} values shown in Fig. 8 are lower than the corner Cp value from the NBCC data. With all of these test data, two important observations can be summarized:

(1) Generally, the Cp_{peak} values collected from the wind tunnel data are found to be smaller compared to that of the maximum CpCg value from NBCC (2005). This provides a level of confidence in the use of the data for further analysis.

(2) It is evident that the roof aspect ratio, building height presented in terms of H/W ratio and approaching wind angle are significantly influence the wind-induced pressure fluctuations. These influences should be considered in such a way when using the wind tunnel data to establish load cycles for the wind uplift resistance evaluation of rigid membrane-roofing systems. One way to deal with this is by always considering the pressure time histories data for the analysis from the worst case scenario occurs during wind actions on roof.

2.3 Rigid vs flexible roof responses

2.3.1 Pressure time histories of PVC, EPDM and rigid models

Fig. 9 shows typical examples of pressure time histories from the rigid and flexible models. The pressure time histories shown in Fig. 9 are taken from similar location (corner roof zone) and tested under open country exposure with 45 degree wind angle for the building height (H) / building width (W) ratio equal to 1. It is noted that the present study used the previously established wind tunnel data to investigate difference in system response between flexible (Baskaran *et al*. 1996, Savage *et al*. 1996, Baskaran *et al*. 1997, Baskaran *et al*. 1999) and rigid roofs under wind-induced pressures. Despite efforts were made when comparing the data, it was realised that both models were tested at different model scale and at different wind tunnel facilities. Although, the current models were performed under the same terrain condition, open country exposure, other differences in terms of pressure tap layouts could affect the results due to possible Reynold numbers variation between the two wind tunnel studies. Further research using the same model configurations (flexible and rigid roofs) and the same wind facility is necessary to validate the results presented herein. To perform direct comparison between flexible and rigid roofs, wind tunnel testing using rigid model can be conducted at the NRC's wind tunnel test facility following similar configurations to that of the flexible model.

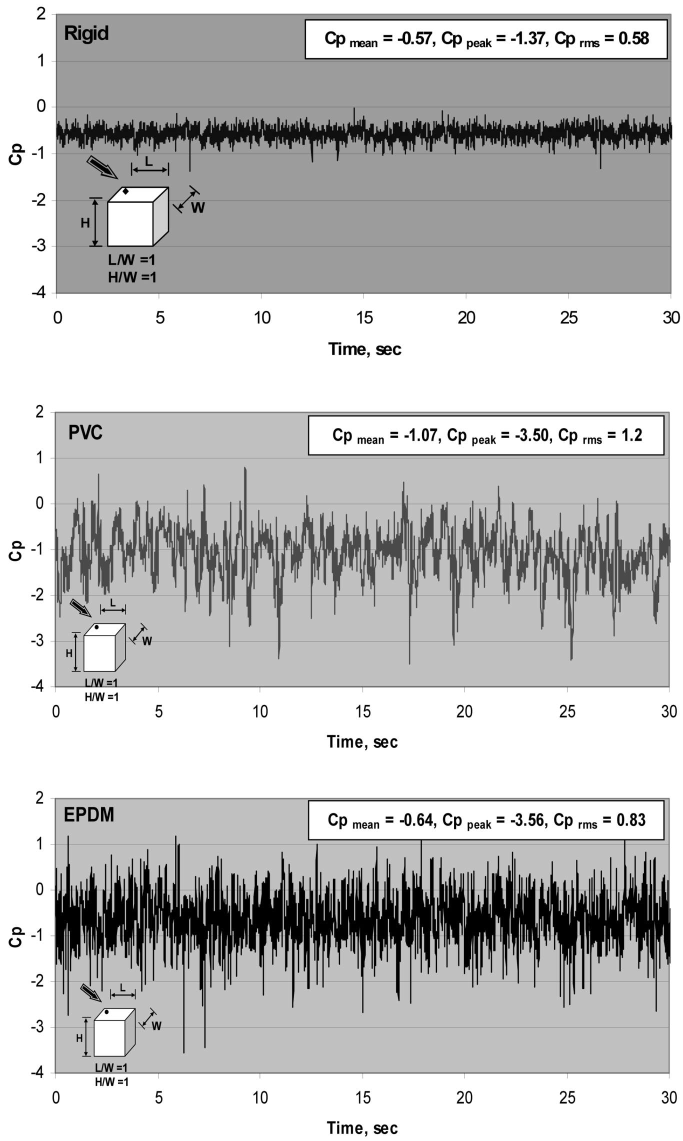

Fig. 9 Pressure time histories for rigid and flexible (PVC & EPDM) models

Due to the data availability, comparison of the pressure time histories was made up to the 30 seconds duration. The mean, peak and rms values from the three pressure time histories data were calculated and plotted in the graphs as shown in Fig. 9. Savage *et al*. (1996) illustrated that the simulated wind tunnel model had a time scale of 1:51 compared to full-scale. This also means that 1 second in the wind tunnel is equal to 51 seconds at the full-scale condition. Based on this understanding, the pressure coefficient time history data used to study roof system response represents the full-scale windstorm condition for 1530 seconds. Extensive comparative study carried out in the past with the field data indicates that duration of 900 seconds would be sufficient for causing about 75% of the damage on roofing systems (Jancauskas *et al.* 1994). With this in mind, the rigid model data collected from this wind tunnel study for a period of 1530 seconds have sufficient length to cause damage on substantial part of the roofing systems.

By only using information presented in Fig. 9, such as the mean, peak and rms of the pressure time histories, are not enough to find out the significant data variation differences and predominant frequency between flexible and rigid roofs. In order to further study the system response between rigid and flexible roofs, probability distribution function (PDF) and spectra analysis were used as analysis tools to explain the responses by using the available pressure time histories data from both models. Further information for both analyses can be found in Murty (2009). The summary of the PDF and spectra analysis are described below,

2.3.2 Probability distribution of the system response

To understand the system response, the use of the PDF is only focused for studying pressure time history data variation between rigid and flexible roofs. Understanding the pressure time history data variation of rigid and flexible roof is important since it can provide an idea about the variation of suction fluctuations due to aerodynamic forces during wind actions. Three sets of Cp data represent the corner, perimeter and field roof zones of the rigid and flexible roofs were selected. Fig. 10 shows typical examples of probability distribution comparison between flexible and rigid roofs for the three different roof zones with H/W = 1. From the PDF analysis, the following conclusion can be drawn:

· The variation of the Cp data for flexible roof is higher than the Cp data for rigid roof. The variation is caused by the method of attachment used for the membrane. The flexible roofs use membranes that are attached using fasteners to substrate at discrete locations. This cause the membranes to flutter during wind action compared to rigid roof. The fluttering effect creates higher Cp data variation that represents suction fluctuations on roofs. In the case for rigid roof, the membranes are adhered to the substrates such as on Adhesive Applied Roofing Systems (AARS). AARS is a type of roof that only use adhesive as method of attachment for its components (Murty 2009). In the AARS, membrane fluttering do not exist hence create lower Cp data variation. The Cp data variation can influence the number of cycles (gusts) used for the load cycles.

· The PDF of the Cp data series found in this study were non-Gaussian as the curves are negatively skewed especially at the corner and perimeter zones, while at the field zone the rigid data series seems to be Gaussian and for the flexible data series was non-Gaussian.

· The probability densities of Cp data set from higher to lower rating grouped by roof locations were corner, perimeter and field zones

2.3.3 Spectral analysis of the system response

The spectral analysis was performed to study the difference in response and to investigate the predominant frequency for the peak energy of pressure time history data between rigid and flexible roofs. Finding the predominant frequency for the peak energy of pressure time history data between rigid and flexible roofs is important since it gives an identification of the time period when the peak energy of wind-induced pressure occurs. For the comparison, three sets of data representing three different roof zones, namely corner, perimeter and field, were selected from the rigid and flexible data. The three sets of data used for this analysis were chosen from similar tap locations, model heights, roof aspect ratios and the wind angle. The PSD computations were performed by the developing a program using Matlab Version 7.0.1, Mathwork Inc (2004). The Matlab program uses the Burg algorithm that incorporates the Fast Fourier Transform algorithm to obtain the power

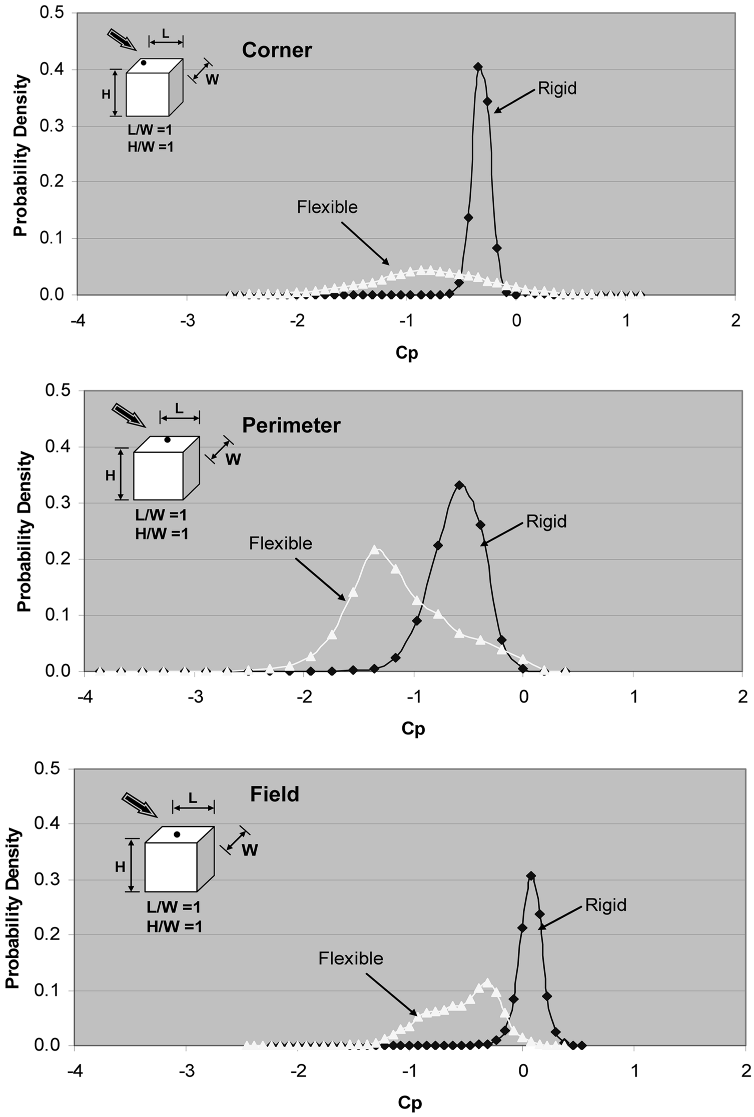

Fig. 10 PDF of wind pressure for rigid and flexible roofs at the three different zones (H/W = 1)

spectral density and the analysed data also plotted to give visual representation. To represent a data for the flexible roof, the PSD computation data from the two types of flexible membrane were averaged. Fig. 11 shows an example of the PSD function of rigid and flexible roofs for the three different zone with H/W=1. In view of the fact that the maximum of the PSD values were observed at the lower frequency range, only a cut off frequency up to 10 Hz was used for this comparison. From the spectra analysis, the following information is obtained.

· Spectral peaks of the flexible roof are found always consistently higher than those of the rigid roofs, regardless of the roof locations.

· The PSD peaks of both flexible and rigid models are higher in the sequence of the corner, perimeter and field roof zones.

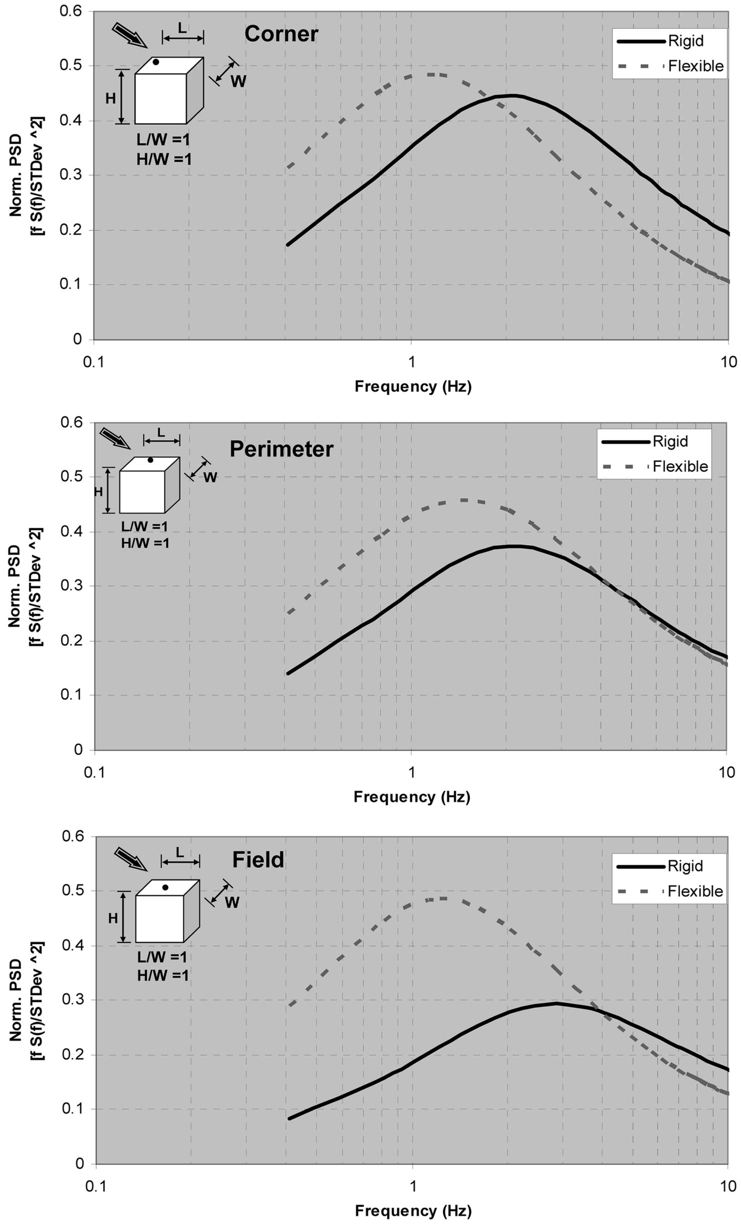

Fig. 11 PSD function of rigid and flexible roofs for the three different zone (H/W = 1)

· The PSD peaks recorded for both models were occurred at the frequency lower than 4 Hz.

From both PDF & PSD analysis and observations, it is clear that the system responses of the rigid and flexible roofs due to wind actions are different. The difference in roof system responses due to membrane fluttering affects wind-induced suction fluctuations on roof and it eventually influences the wind uplift resistance. Hence the "CSA A123.21-04" needs to be modified to incorporate the rigid response due to wind actions on roof. It also means that a new load cycle is required for the wind uplift resistance evaluation of rigid membrane-roofing systems.

3. Computation of load cycle using rain flow counting

As previously mentioned, the CSA A123.21-04 uses SIGDERS load cycles as a loading method during testing to represent simplification of wind-induced pressure fluctuations on roof. However, the load cycles for wind uplift resistance evaluation presented in CSA A123.21-04 can not be used to evaluate wind uplift resistance for rigid roofs. This is due to the fact that rigid roof response during wind action is different in comparison to that of the flexible roofs. The development of load cycles for rigid roof herein follows a similar procedure to that of SIGDERS load cycles. The dynamic responses of measured suction coefficients from 270 time histories data were converted into discrete response using the rain flow counting (RFC) method to account for wind-induced suction fluctuations that eventually produces fatigue effect on roofing systems. The RFC method has been proven to be a good method for predicting the fatigue effects of a random process (Downing and Socie 1982, Rychlik 1987, Glinka and Kam 1987 and Amzallag *et al*. 1994). The RFC method has also been used by ASTM E1049-2005 as a standard practice for cycle counting in fatigue analysis. Detailed explanation and an example for the use of RFC method for the prediction of wind-induced fatigue loading on roofs is found elsewhere, Xu (1995). For the purpose of the load cycle computation for rigid roof, the previously developed RFC computer program (Baskaran *et al*, 1997) was used to predict the wind-induced fatigue loading on the rigid model test data. The RFC method was rewritten using the Compaq Visual FORTRAN Version 6.6 (2001). Details of the RFC computer program used in this study can be found in Chen and Baskaran (1997). For the data analysis, the 270 time histories of measured suction coefficients were categorized into 18 groups. They consist of 9 groups of data under the wind direction of 0 degree, for three roof aspect ratios (L/W) and three building heights over width ratios (H/W). The other 9 groups are for the same configurations under the 45 degree wind. The following four-step procedures were performed.

1. Classification of the time histories of measured pressure coefficients under the same group conditions, for example, the same L/W ratio, H/W ratio and wind approaching angle.
2. Application of the RFC method
3. Counting the number of cycles for each pressure tap
4. Identification of the maximum number of cycles under the same group condition.

The outcome of the data analysis by following the above procedure was presented in terms of a 10 by 10 matrices that describes the occurrences of certain suction coefficient on the test data considered as shown in Table 2. Typical example of calculation overview to obtain result as shown in Table 4 is described in Appendix 1. **M** in the rows represents the **M**ean normalized suction coefficient values, whereas **R** in columns signifies the **R**ange of normalized suction coefficient values, while the values in the column matrix identify the calculated maximum number of cycles. Both M and R are tabulated from 0 to 1 with the increments of 0.1. As mentioned previously the 15 pressure taps were installed on the rigid models during wind tunnel testing to measure the dynamic system response. By combining the 10 × 10 matrices from the 15 individual pressure taps, another 10 by 10 matrices for a specific tested group condition was developed. The combining 10 × 10 matrices represents the maximum number of cycle for the above specific group condition. Table 2 and Table 3 provide typical examples of the combined 10 × 10 matrices for the group with L/W and H/W ratios of 1. The data in Table 2 present the maximum number of cycles for the wind angle of 0 degree, while Table 3 represents the data for the 45 degrees wind angle. The values in columns and rows refer to the occurrence of number of cycle measured. For example, in the M1 (row) and

Table 2 Typical M × R matrix (L/W = 1; H/W = 1; Wind = 0 degree)

	R1	R2	R3	R4	R5	R6	R7	R8	R9	R10
M1	0	0	57	11	1	0	0	0	0	0
M2	0	0	67	20	5	2	0	0	0	0
M3	0	0	131	74	25	11	1	0	0	0
M4	0	0	131	46	54	27	7	1	0	0
M5	0	0	14	13	3	0	1	2	2	0
M6	0	0	2	1	0	0	0	0	0	0
M7	0	0	0	0	0	0	0	0	0	0
M8	0	0	0	0	0	0	0	0	0	0
M9	0	0	0	0	0	0	0	0	0	0
M10	0	0	0	0	0	0	0	0	0	0

Table 3 Typical M × R matrix (L/W = 1; H/W = 1; Wind = 45 degree)

	R1	R2	R3	R4	R5	R6	R7	R8	R9	R10
M1	0	0	1	0	0	0	0	0	0	0
M2	0	0	85	73	6	0	0	0	0	1
M3	0	0	121	132	85	25	2	0	0	0
M4	0	0	121	45	52	65	56	36	4	0
M5	0	0	27	32	12	11	10	6	17	11
M6	0	0	21	6	4	1	2	1	0	7
M7	0	0	3	2	4	0	1	0	0	0
M8	0	0	3	3	0	0	0	0	0	0
M9	0	0	1	1	0	0	0	0	0	0
M10	0	0	0	0	0	0	0	0	0	0

Table 4 Typical M × R matrices (L/W = 1; H/W = 1)

	R1	R2	R3	R4	R5	R6	R7	R8	R9	R10
M1	0	0	57	11	1	0	0	0	0	0
M2	0	0	85	73	6	2	0	0	0	1
M3	0	0	131	132	85	25	2	0	0	0
M4	0	0	131	46	54	65	56	36	4	0
M5	0	0	27	32	12	11	10	6	17	11
M6	0	0	21	6	4	1	2	1	0	7
M7	0	0	3	2	4	0	1	0	0	0
M8	0	0	3	3	0	0	0	0	0	0
M9	0	0	1	1	0	0	0	0	0	0
M10	0	0	0	0	0	0	0	0	0	0

R3 (column) of Table 2, 57 occurrences of number of cycle was computed for the 0 degree wind where each occurrence has a mean value of 0.1 (M1) and a range from 0.2 to 0.3 (R3). It is noted when calculating the number of cycles, a low-pass filter of 5% of the maximum suction coefficient was applied. From Table 2 and Table 3, it is noticeable that the number of occurrence with 0 degree wind is mostly low compared to the data with 45 degree wind for the same mean and range of the normalized suction coefficient values. This implies that wind-induced pressure fluctuation is higher and as a result of this, the roofing system receives more fatigue damage for the oblique wind direction. In addition, the distribution of the number of occurrence in terms of 10 × 10 matrices for the data with the 0 degree wind direction was more localized compared to the 45 degree wind.

For further analysis, simply the greater number of occurrence for the same mean and fluctuation of 10 × 10 matrices was taken for each specific area. By doing so, the data used for further analysis represent the worst case scenario for each area of the roof. The result would be more conservative than being accurate but it is consistent with the conventional approach often taken by any design standards. At the end, one can obtain the maximum number of cycles for each data group corresponding to the respective mean and range pressures. Table 4 presents typical example of the 10 × 10 matrices for the data with the L/W and H/W ratios of 1. The 10 × 10 matrices data in Table 4 was calculated based on the data presented in Table 2 and Table 3. For example, the number of occurrence for the M2R3 of Table 2 (0 degree) and of Table 3 (45 degree) is 67 and 85, respectively. Thus the number of occurrence used for the M2R3 in Table 4 is 85 by taking the greater number. To develop the dynamic load testing procedure for the rigid membrane-roofing systems evaluation, the 10 by 10 matrices data were reorganized into eight different pressure zones with their respective number of cycles. The eight pressure zones were selected under two groups as follows,

· Group 1: N1 (0.0 - 0.25), N2 (0.0 - 0.5), N3 (0.0 - 0.75), N4 (0.0 - 1.0), and

· Group 2: N5 (0.25 - 0.5), N6 (0.25 - 0.75), N7 (0.25 - 1.0) and N8 (0.5 - 1.0)

The number of cycles for each zone was then gathered. The action was performed by examining each cell of the M by R matrix. If the combination of means and range pressure falls into a particular zone, then the cycles were counted for that pressure zone (Ns). The following procedures are used for the reorganization and a typical example of the calculation process is also presented in parenthesis corresponding to the data for the cell M1R3 of Table 4.

1. Calculate the highest range of suction pressure for the cell, (for M1R3, it is 0.3).

2. Calculate the lowest mean of suction pressure for the cell, (for M1R3, it is 0).

3. Determine the lowest suction pressure that is encountered by the cell. It is the lowest mean of suction pressure value subtracted by a half of the highest range of suction pressure, (for M1R3, it is 0-0.03 = 0, if negative is equal to zero).

4. Calculate the highest mean of suction pressure for the cell (for M1R3, it is 0.1).

5. Determine the highest suction pressure that is encountered by the cell. It is the highest mean of suction pressure value added by a half of the highest range of suction pressure, (for M1R3, it is 0.1+0.15 = 0.25).

6. Determine the suction pressure zone based on the suction pressure variation calculated in procedures 3 and 5, (for M1R3, it falls into the $N1$ suction pressure zone [0.0-0.25]).

7. Calculate the total number of cycles from all cells that correspond to a particular suction pressure zone, (M1R1, M1R2, M1R3 and M2R1 contribute to $N1$ for a total of 57 cycles [0+0+57+0] of the Group 1, Fig. 12).

A computer program by Compaq Visual FORTRAN Version 6.6 (2001) has been developed to aid the calculation process (Murty 2010). Fig. 12 shows a typical load cycle for Group 1 thus calculated. The number of cycles for N2, N3 and N4 was calculated by a similar procedure as for N1, supported by the program. Fig. 13 depicts typical load cycles thus calculated for Group 2 that consists of four sequences namely, N5, N6, N7 and N8. The Groups 1 and 2 of Figs. 12 and 13, respectively, were obtained using the data presented in Table 4. By comparing Figs. 12 and 13, it is noticed that the number of cycles for the Group 1 is significantly higher in comparison to the Group 2 and the number of cycles recorded for the N5 is equal to zero. This means that there is no system response recorded that has a suction pressure range of 0.25 – 0.5 during testing. This reflects that the tested rigid models have different wind-induced response compared to the flexible roofs.

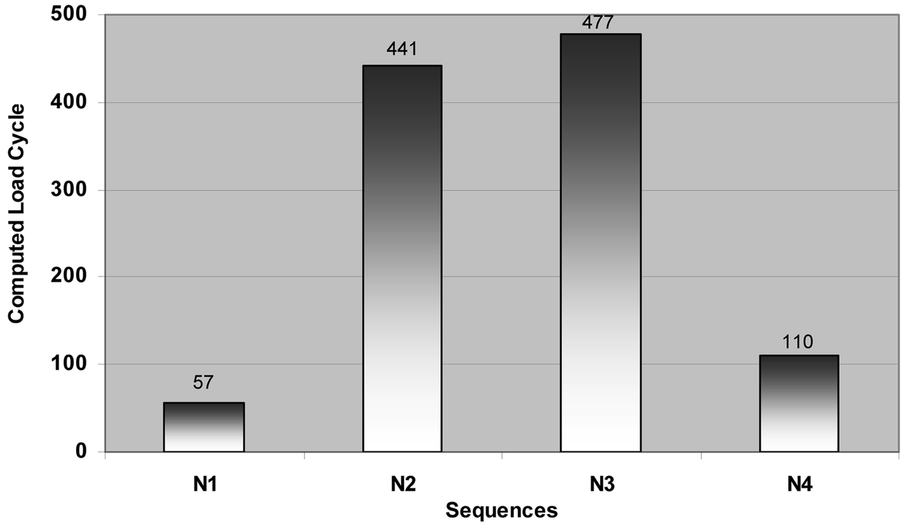

Fig. 12 Computed load cycle for group 1

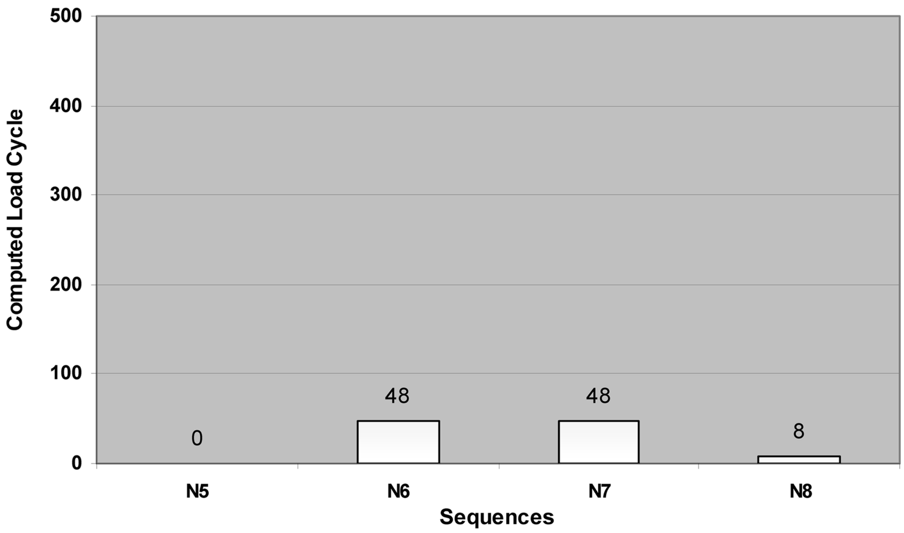

Fig. 13 Computed load cycle for group 2

4. Development of load cycle for rigid roofs

To develop a generalised load cycles for the evaluation of the rigid roof system, a similar computational procedure as described in the previous section was applied for different configurations of the wind tunnel data. The outcome is presented in Table 5. The summarized load cycle data were computed by using 270 time histories of measured suction coefficients on the rigid models. They were classified into three different building heights and three different aspect ratios. It was noticed that the effects of difference in H/W and L/W ratios on the data were minimum as shown in Table 5. However, the extreme load cycles were selected as highlighted at the bottom of Table 5 for further data analysis. The development of load cycles for rigid roof evaluation requires several levels of generalization of the wind effects over a roof assembly that warrants compromise from the technical approach to the practically acceptable procedures. It means that the developed load cycle should consider several conditions such as follows:

· Simulation of natural wind effects as realistically as possible;
· Simulation of the failure modes comparable to the field observation;
· Easiness of application in a common laboratory environment;
· A short testing time, not more than a day including the preparation time, for all practical purposes; and
· Compatibility with the local building codes and wind standards.

Considering the above conditions, the extreme load cycles for rigid roof presented in Table 5 have been simplified by studying ratios between the established SIGDERS load cycles for the flexible roofs with the original SIGDERS data tested in the wind tunnel. Fig. 14 compares the extreme load cycle data of the two roof models. The top bar charts illustrates the number of calculated load cycles comparison for Group 1 that consists of N1 to N4 while the bottom bar charts provides the data for N5 to N8 of Group 2. Using the data presented in Fig. 14, the load cycles for rigid roof were developed. Computation of N1 to N8 of the Level A, load cycles for rigid roof is performed

Table 5 Summary of computed load cycle group 1 and 2 for all model data tested

L/W ratio	H/W ratio	Number of gusts							
		Group 1				Group 2			
		N1	N2	N3	N4	N5	N6	N7	N8
	1	57	441	477	110	0	48	48	8
1	2	29	419	452	207	0	71	82	11
	3	39	453	480	241	0	73	109	13
	1	40	504	487	73	0	31	22	0
2	2	55	403	475	174	0	133	107	5
	3	18	406	437	238	0	126	167	16
	1	37	446	478	77	0	106	80	2
0.5	2	35	321	244	23	0	10	9	0
	3	35	315	191	9	0	5	4	0
Extreme load cycle for rigid roof		57	504	487	241	0	133	167	16

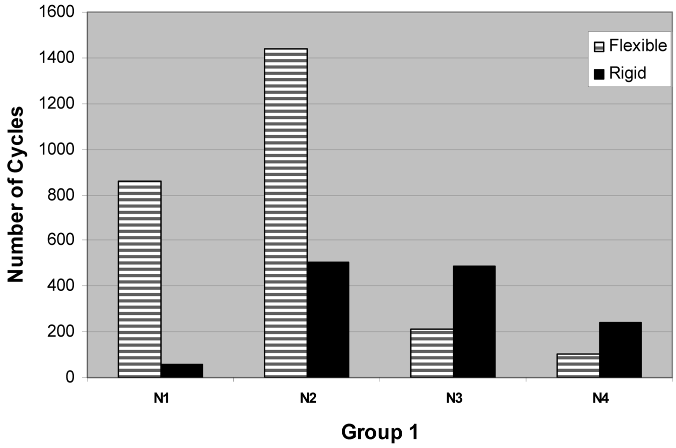

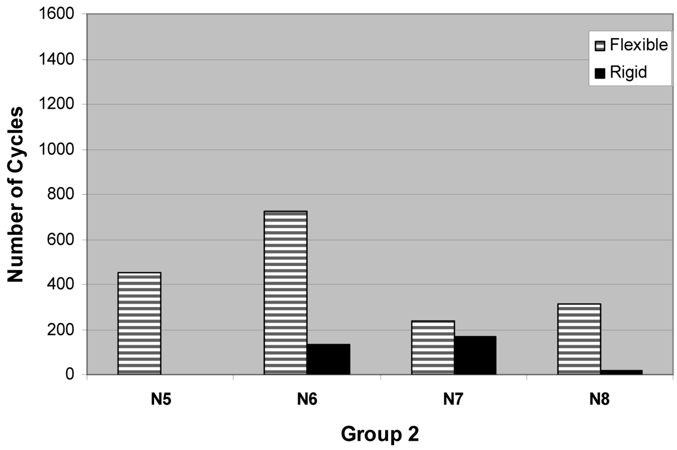

Fig. 14 Load cycles comparison between the flexible and rigid roof models

using the following way

$$NR_{std} = (\ NF_{csa} / NF_{WT}\ ) \times NR_{WT} \tag{1}$$

Where,
NR_{std} = Calculated Number of Load Cycles for a N Rigid –Sequence
NF_{csa} = CSA Number of Load Cycles for a N Flexible -Sequence (Level A - Fig. 4)
NF_{WT} = Number of Load Cycles for a N Flexible –Sequence based on Wind Tunnel Test.
NR_{WT} = Number of Load Cycles for a N Rigid –Sequence based on Wind Tunnel Test. Example: The number of calculated load cycles for the N1 - Rigid (N_1R_{std}) is 26 [(400 / 863) × 57].

Table 6 summarizes the number of load cycles for the rigid roofs obtained using the above mentioned steps and named as "Considered Level A of Load cycles for Rigid Roof". The "Considered Level A of Load cycles for Rigid Roof" was later used as the basis for establishing the level A of the dynamic rigid load cycles. It was noted that all values of NR_{std} 's were calculated

Table 6 Considered level A - dynamic load cycle for rigid roof

Seq.	Load cycles raw data-flex		Avg. of lc-flex (NF_{WT})	Flex load cycles-CSA (NF_{csa})	Load cycle raw data-Rigid (NR_{WT})	Ratio of NF_{csa}/NF_{WT}	Calculated load cycles-Rigid (NR_{std})	Level A-considered load cycle-Rigid
	PVC	EPDM						
N1	850	875	863	400	57	0.46	26	26
N2	1300	1575	1438	700	504	0.49	245	245
N3	225	200	213	200	487	0.94	458	458
N4	80	125	103	50	241	0.49	118	50
N5	380	525	453	400	0	0.88	0	0
N6	425	1025	725	400	133	0.55	73	73
N7	50	425	238	25	167	0.11	18	18
N8	25	600	313	25	16	0.08	1	1

using the above method, an exception have been made only for the N_4R_{std} that 50 number of load cycles are maintained. The decision to maintain the N_4R_{std} - number of load cycles similar to the N_4R_{csa} -SIGDERS number of load cycles have been discussed with the input from AARS project members. The selected number of load cycles (50) is also believed to have represented enough fatigue effects on the system during testing. The "Considered Level A of Load cycles for Rigid Roof " consists of eight load sequences (N1 to N8) with different pressure ranges as shown in Fig. 15. The vertical axis represents the percentage of the maximum pressure applied on each sequence of Level A. The maximum pressure corresponds to the design pressure prescribed in building codes or wind standards. The eight sequences (*X* axis) were divided into two groups. Group 1 represents the wind-induced suction over the roof assembly that consists of four sequences (N1 to N4) where the pressure level alternates between zero to a fixed pressure. Group 2 characterizes the effect of exterior wind fluctuations combined with a constant interior pressure on a building. The effect of internal pressure variations were codified in the North American wind standards (ASCE 2010, NBCC 2010). In the Group 2, a constant minimum static pressure is applied and the pressure level alternates between this minimum and the maximum pressures for each sequence. To be conservative, a time period of 8 seconds is selected to complete one gust/cycle loading. The 8 seconds period duration is divided into 2 sequences, loading and unloading. The duration of these 2

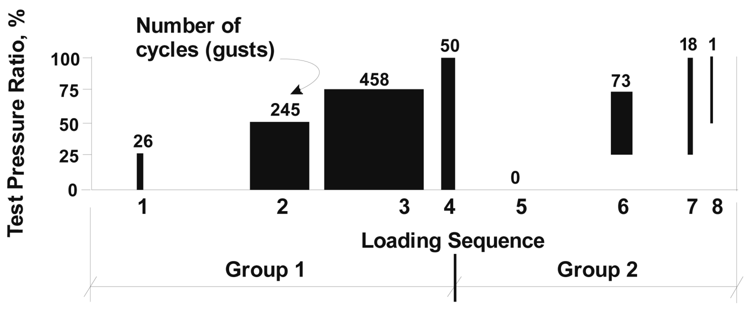

Fig. 15 Dynamic load cycles for the rigid roof evaluation

sequences are minimum of 2 seconds or longer. This time period was longer than the time period observed during the PSD analysis of wind-induced pressure of the rigid roof. As described in previous section, the predominant frequency of wind-induced pressure for the rigid roof was observed ranging from 2 Hz to 4 Hz. This means that a minimum time period of 0.5 seconds is required. Other reason for the selection is to have similar time period with the CSA A123.21-04 load cycle for possible testing data comparison between rigid and flexible roofs. Fig. 16 shows the time required to complete the one gust/cycle for Group 1 and Group 2 of Fig. 15.

4.1 Generalization of load cycle for rigid roofs

In order to evaluate the ultimate wind uplift resistance of a roofing system, that is of major importance to roofing manufacturers for comparing their product with others, a method of load cycle generalization has been developed. The generalization is required due to the fact that the load cycle for rigid roof presented in Fig. 15 may not be able to provide this information. To understand this, let us consider a particular situation of a roofing manufacturer who selected a system and

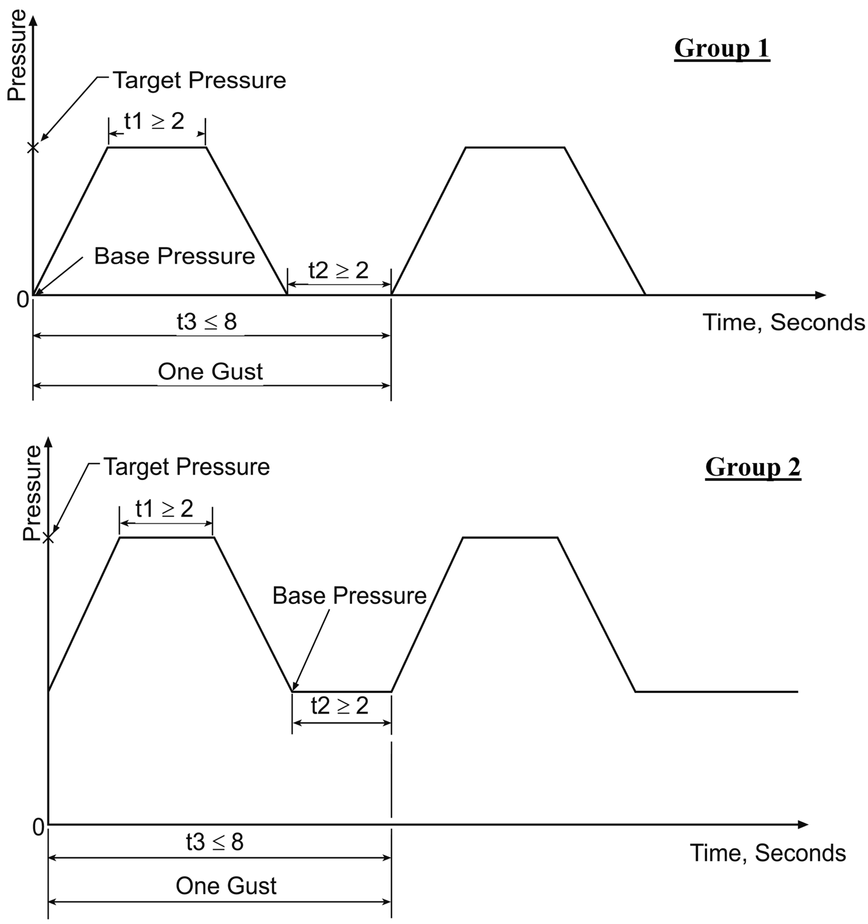

Fig. 16 Time requirement for one gust (cycle)

tested it with test pressure of 60 psf (2.87 KPa). According to Fig. 15, if the system successfully passes all the load cycles, it can be certified as P_{60}. However, in this scenario, the client is not aware of the ultimate strength of the tested roofing system. On the other hand if the system's failed before passing all the load cycles, the manufacturer is required to redesign the system components. Thus, the developed load cycle is useful for those who have a clear understanding of their system strength or for those have tested similar systems in the past. Based on the past experience, they can select the appropriate test pressure for which the system can pass all the required cycles at the selected test pressure level. It is not a viable solution when new products / installation procedures are constantly evolving. To overcome this situation, the method of load cycle generalization for rigid roof was introduced by utilizing ratios of the SIGDERS (CSA) load cycles to forecast the number of load cycles at pressure levels that were not tested in the wind tunnel. The following procedure describes an example of using the ratios method to forecast the load cycles of rigid roof for the Sequence N1 to N8 of Level B to Level E.

1. Calculate the ratio of N2-Level B to N2-Level A of the CSA load cycles = 0.71 [500 (N2-Level B) / 700 (N2-Level A) = 0.71]. Table 7 encapsulates all of the calculated ratios from SIGDERS (CSA) load cycles for the determination of load cycles for rigid roof.
2. Establish the N2 – number of cycle of the Level B for rigid roof by multiplying the obtained ratio (0.71) with the N2 of Fig. 15 [0.71 × 245 = 175]

By adopting a similar procedure as N2 Level B other values of N2 for Level C to Level E were calculated as well as other sequences for Level B to Level E. The completed calculation results are tabulated in Table 8. For the rigid system, the performed calculations provide the total number of cycles of 652, 555, 395 and 368 for the Level B, Level C, Level D and Level E respectively.

4.2 Proposal of load cycle for rigid roofs

The calculated dynamic rigid load cycles presented in Table 8 were simplified and the values were rounded up or down to the nearest number of load cycles as presented in Table 9. Following the number of load cycle simplifications, the load cycles shown in Table 9 was proposed to use for

Table 7 Calculated ratios for the different levels to the level A of CSA load cycles

Group #	Loading sequence	Level A	Level B		Level C		Level D		Level E	
		Cycles	Cycles	Ratio to A	Cycles	Ratio to A	Cycles	Ratio to A	Cycles	Ratio to A
1	N1	400	0	0.00	0	0.00	0	0.00	0	0.00
	N2	700	500	0.71	250	0.36	250	0.36	200	0.29
	N3	200	150	0.75	150	0.75	100	0.50	100	0.50
	N4	50	50	1.00	50	1.00	50	1.00	50	1.00
2	N5	400	0	0.00	0	0.00	0	0.00	0	0.00
	N6	400	350	0.88	300	0.75	50	0.13	0	0.00
	N7	25	25	1.00	25	1.00	25	1.00	25	1.00
	N8	25	25	1.00	25	1.00	25	1.00	25	1.00
	Total =	2200	1100		800		500		400	

Table 8 Calculated dynamic load cycle for rigid roof based on CSA load cycle ratios

Group #	Loading sequence	Number of cycles proposed				
		Level A	Level B	Level C	Level D	Level E
1	N1	26	0	0	0	0
	N2	245	175	88	88	70
	N3	458	344	344	229	229
	N4	50	50	50	50	50
2	N5	0	0	0	0	0
	N6	73	64	55	9	0
	N7	18	18	18	18	18
	N8	1	1	1	1	1
	Total =	872	652	555	395	368

Table 9 Number of cycles at the 5 levels

Group #	Loading sequence	Number of cycles proposed				
		Level A	Level B	Level C	Level D	Level E
1	N1	25	0	0	0	0
	N2	250	175	100	100	75
	N3	450	350	350	225	225
	N4	50	50	50	50	50
2	N5	0	0	0	0	0
	N6	75	50	50	0	0
	N7	20	20	20	20	20
	N8	5	5	5	5	5
	Total =	875	650	575	400	375

the wind uplift resistance evaluation of rigid membrane-roofing systems. Under the proposed load cycles, the testing time required to complete Level A is less than 2 hours. While the total duration time required for completion of all levels (Level A to Level E) is less than 6.5 hours. The total number of cycles to complete the five levels is 2886 cycles. This total number of cycles is about 40% less than the total number of CSA (flexible) load cycles and the 40% less number of cycle results in a reduction of testing time of about 4.5 hours. Fig. 17 presents the two load cycles for the dynamic wind uplift resistance evaluation of roofing systems. Method 1 and Method 2 are used for the wind uplift resistance evaluation of flexible roof and rigid roof, respectively. It is noticed that the number of cycles for Method 1 of Fig. 17 is same as Fig. 4, while Method 2 of Fig. 17 is the newly developed load cycle. The newly developed load cycle for the wind uplift resistance evaluation of rigid membrane-roofing systems presented in Method 2 consists of five levels (A, B, C, D and E) and each level has eight sequences (N1 to N8). Similar to SIGDERS (CSA A123.21-04) load cycles, the rating is established when all specified numbers of cycles in each level have been completed without any resistance link failures. The proposed load cycles can provide various options for the roofing community. Two of them are summarized as follows,

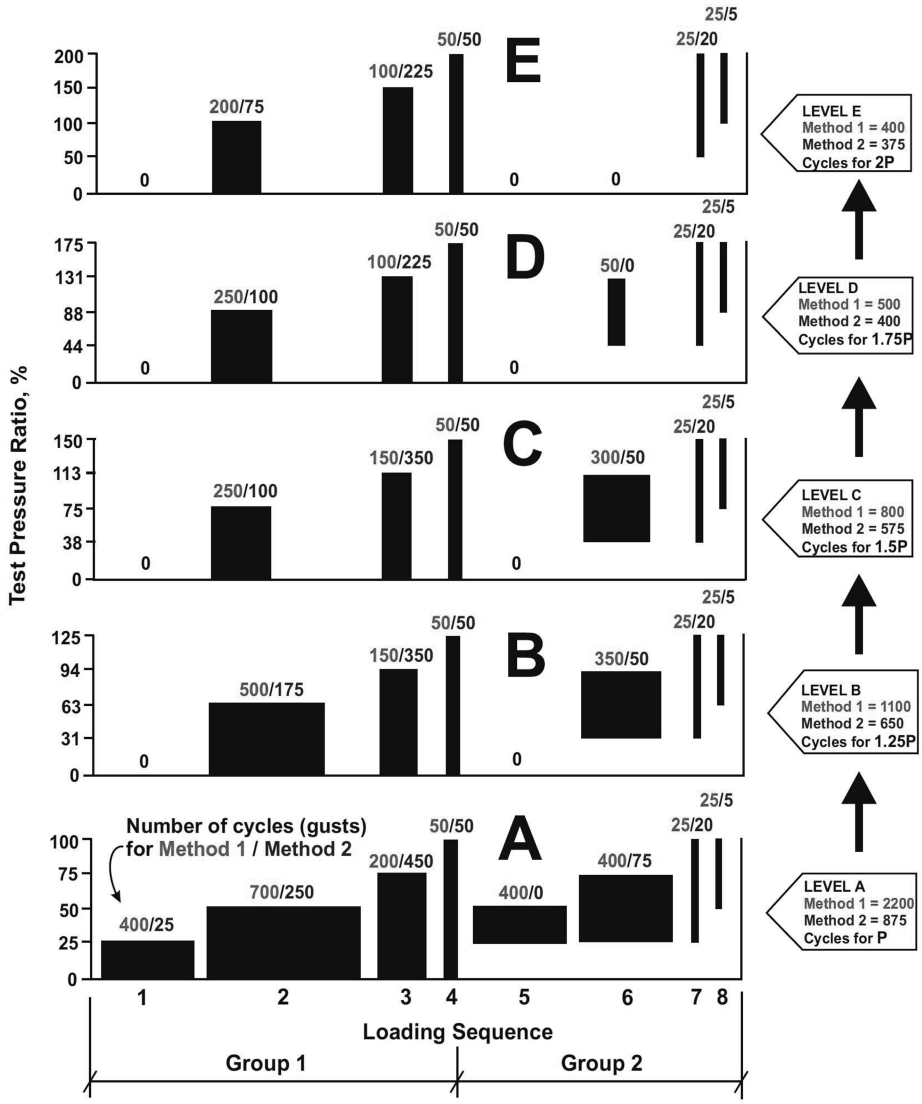

Fig. 17 Revised load cycle for the wind uplift resistance evaluation of membrane roofing systems (method 1 and method 2)

4.2.1 Option 1: Introduction of safety factor in system design

The load cycle for rigid roof was developed to satisfy the regulatory requirements. The design pressures are used to convert the ratios on the ordinate of Fig. 17 and such pressures are established in accordance with the local wind standards or building code minimum requirement recommendations. Systems that pass level A can be tested with the design pressure increased incrementally by 0.25. Thus it can provide roofing manufacturers with the safety factor, while the building codes or wind standards prescribe only "minimum design values." The proposed load cycle distribution presents the safety factor of 2 for the design pressure. Group 1 represents the wind-induced suction over a roof assembly. It consists of four sequences, where the pressure level alternates between zero and a fixed pressure. Group 2 represents the effects of exterior wind fluctuations combined with a constant interior pressure on a building.

4.2.2 Option 2: System rating certification

This option provides roofing manufacturers for system rating. The system rating certification is needed to ensure that roofing system meets the minimum design pressure prescribed in the building code requirements. The process of system rating certification can be used to quantify either a new roof assembly or to verify a roof assembly due to new substitution or enhancement of components. The rating can be established when the system tested complete all sequences on each corresponding level. The established rating is used to determine whether or not, a roofing system can be installed at a specific location. This is performed by dividing the rating's with the factor of safety and compare this value with the design wind uplift pressure values (corner, edge and field) obtained from the building code (e.g., NBCC 2010, ASCE-07 2010). To use roofing system at specific location, the pressure rating's value should be larger than design wind uplift pressure values obtained from the building code.

5. Conclusions

The present paper compared the wind performance of rigid and flexible roofs. Analysis of the pressure time histories data using probability distribution function and power spectral density verified that these two roofs types exhibited different system responses under wind forces. The difference in roof system response provided clear understanding that each type of roofing system should be assessed differently to better predict their wind uplift resistance performances. The load cycle for the wind uplift resistance evaluation of rigid roofing system was developed using wind tunnel data by applying rain flow counting method. The developed load cycle had also been generalized and extended to evaluate the ultimate wind uplift resistance capacity of rigid roofs. During review process of this paper, the newly developed load cycle was integrated into the new edition of CSA 123.21-10, as Method 2, for wind uplift resistance evaluation of rigid roofing systems.

Acknowledgments

Financial support was provided by the Natural Sciences and Engineering Research Council (NSERC) project under Grant # CDR 305819. It is a collaborative research and development project with the partners from University of Ottawa, Roofing manufacturers (*BAKOR Inc., IKO Industries Ltd, SOPREMA Inc., TREMCO Inc.),* Roofing Contractor Association of British Columbia (RCABC) and National Research Council of Canada (NRCC).

References

Amzallag, C., Gerey, J.P., Robert, J.L. and Bahuaudl, J. (1994), "Standardization of the rain flow counting method for fatigue analysis", *Int. J. Fatigue*, **16**(4), 287-293.

ASTM E1049 (2005), "Standard practices for cycle counting in fatigue analysis", ASTM International, West

Conshohocken, PA.

ASCE 7 (2010), "Minimum design loads for buildings and other structures", American Society of Civil Engineer (ASCE), Reston, VA.

Baskaran, A. (1986), *Wind load on flat roofs with parapet* , MEng. thesis, (Building), Centre for Building Studies, Concordia University, Montreal,QC.

Baskaran, A, Savage, M.G., Alfawakhiri, F and Cooper, K (1996), *Pressure distribution data measured during the october 1995 wind tunnel tests on a mechanically attached EPDM single ply roofing systems*, Internal Report LTR A004, Institute for Aerospace Research (IAR), NRCC, 1-203, Ottawa, ON, Canada.

Baskaran, A., Chen, Y and Savage, M (1997), "Development of a wind load cycle for testing commercial building envelopes", *Proceedings of the Struct. Congress XV,* ASCE, Portland, Oregon.

Baskaran, A., Chen, Y. and Vilaipornsawai, A (1999), "A new dynamic wind load cycle to evaluate flexible membrane roofs", *J. Test. Eval*., **27**(4), 249-265.

Banks, D., Meroney, R.N., Sarkar P.P., Zhao and Z., Wu, F. (2000), "Flow visualization of conical vortices on flat roofs with simultaneous surface pressure measurement" , *J. Wind Eng. Ind. Aerod.,* **84**(1), 65-85.

CSA A123.21-04. (2004), *Standard test method for the dynamic wind uplift resistance of mechanically attached membrane-roofing systems*, Canadian Standards Association (CSA), Toronto, ON.

Chen, Y. and Baskaran, B.A. (1997), *Development of load sequence using pressure records measured from Wind tunnel studies for mechanically attached single-ply PVC and EPDM roofs* , Internal report No. IR743, Institute for Research in Construction, NRCC, Ottawa, ON.

Compaq Visual FORTRAN Version 6.6 (2001), Compaq Computer Corporation.

Downing, S.D. and Socie, D.F (1982), "Simple rainflow counting algorithms", *Int. J. Fatigue*, **4**(1), 31-40.

Glinka, G. and Kam, J.C.P. (1987), "Rainflow counting algorithm for very long stress histories", *Int. J. Fatigue*, **9**(4), 223-228.

Jancauskas, E.D.J., Mahendran, M. and Walker, G.R., (1994), "Computer simulation of the fatigue behavior of roof cladding during the passage of a tropical cyclone", *J. Wind Eng. Ind. Aerod*., **51**(2), 215-227.

Lawson, T.V. (1980), "Wind effect on buildings", *J. Appl. Sci*., **1**, 1-318.

Laaly H.O. (1992), "The science and technology of traditional and modern roofing systems", Laaly Scientific Publisher, 9037, Monte Mar Drive, Los Angeles, CA. , 90035-4235.

Mathwork inc (2004), "Matlab, the language of technical computing", version 7.0.1., Math Software Co., USA.

Murty, B. (2010), *Wind uplift performance evaluation of adhesive applied roofing systems*, Ph.D. Thesis, Department of Civil Engineering, University of Ottawa, Ottawa, Canada, 2009 (in press).

National Research Council Canada (2010), *National building code of canada user's guide-structural commentaries*, NRCC, Ottawa, Canada

Rychlik, I (1987), "A new definition of the rain flow cycle counting method", *Int. J. Fatigue*, **9**(2), 119-121.

Savage, M.G., Baskaran, A., Cooper, K.R and Lei, W. (1996), *Pressure distribution data measured during the November 1994 wind tunnel tests on a mechanically attached, PVC single-ply roofing system* , IAR Report LTR-A-003, NRCC, Ottawa,ON.

Simiu, E and Scanlan, R.H (1986), *Wind Effects on Structures: An introduction to wind engineering*, John Willey & Sons, NY.

Stathopoulos, T., Marathe, R. and Wu, H (1999), "Mean wind pressures on flat roof corners affected by parapets:field and wind tunnel studies", *Eng. Struct*., **21**(7), 629-638.

Stathopoulos, T (2008), *Pressure time histories from rigid wind tunnel models*, Technical Report, Centre for Building Studies, Concordia University. Montreal, QC.

Smith, T.L (2009), "Wind safety of the building envelope, whole building design guide (WBDG)", National Institute of Building Science, Washington, DC.

Uematsu, Y., Watanabe, K., Sasaki, A., Yamada, M. and Hongo, T. (1999), "Wind-induced dynamic response and resultant load estimation of a circular flat roof, closed-type wind tunnel at Kajima Technical Research Institute", *J. Wind Eng. Ind. Aerod*., **83**(1-3), 251-261.

Xu, Y.L., Mehta, K.C. and Reardon, G.F (1995), "Fatigue of metal roof cladding subject to wind loading, part i: fatigue-related characteristics of roof pressures", *Proceedings of the 9th ICWE*, New Delhi. India.

CC

Appendix

This appendix provides typical information on calculating number of occurrences for suction coefficients that are presented in Table 2, Table 3 and Table 4 of the paper. The numbers of occurrences as shown in the above tables were calculated using Rain Flow Counting (RFC) method and it was written in Fortran program. Detailed about the RFC program and calculations can be found in Murty 2010. The steps to account for number of occurrences are given below,

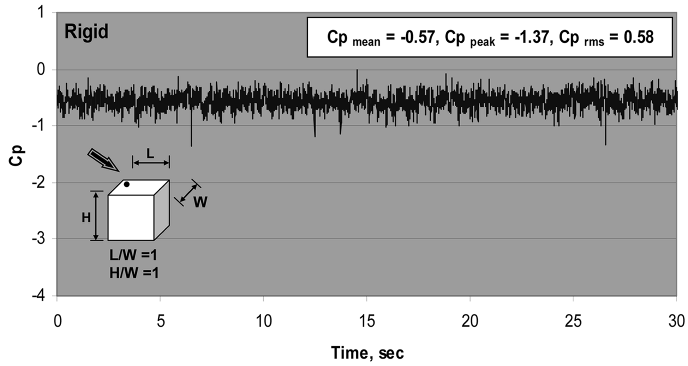

Step 1 Obtain pressure time history data from the wind tunnel testing. *For example*, the time history data for rigid roof model shown in Fig. 9 is used

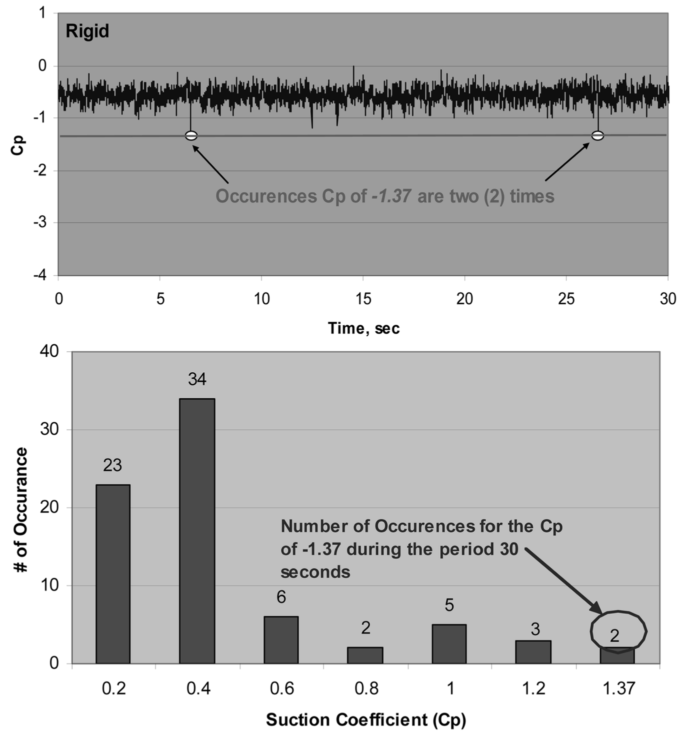

Step 2 Counts number of occurrence using RFC for a suction coefficient from a set of pressure time history data

Note:
Numbers of occurrences in the Bar Chart are not real, it is only for the purpose of presentation.

Counting example:

▶ Range (R) for suction coefficient from 0.2 – 0.4
○ = 23 + 34 = 57
▶ Mean (M) from 0.2 – 0.4
= (0.2 + 0.4) / 2 = 0.2

Step 3 Obtain the occurrence data and present them in term of 10 by 10 matrixes after applying a low-pass filter of 5% and normalizing the suction coefficients with the maximum suction coefficient as shown in Table 2

	R1	R2	R3	R4	R5	R6	R7	R8	R9	R10
M1	0	0	57	11	1	0	0	0	0	0
M2	0	0	67	20	5	2	0	0	0	0
M3	0	0	131	74	25	11	1	0	0	0
M4	0	0	131	46	54	27	7	1	0	0
M5	0	0	14	13	3	0	1	2	2	0
M6	0	0	2	1	0	0	0	0	0	0
M7	0	0	0	0	0	0	0	0	0	0
M8	0	0	0	0	0	0	0	0	0	0
M9	0	0	0	0	0	0	0	0	0	0
M10	0	0	0	0	0	0	0	0	0	0

Step 4. Re-do step 1 to step 3 to attain another set of 10 by 10 matrixes for another wind direction as presented in Table 3

	R1	R2	R3	R4	R5	R6	R7	R8	R9	R10
M1	0	0	1	0	0	0	0	0	0	0
M2	0	0	85	73	6	0	0	0	0	1
M3	0	0	121	132	85	25	2	0	0	0
M4	0	0	121	45	52	65	56	36	4	0
M5	0	0	27	32	12	11	10	6	17	11
M6	0	0	21	6	4	1	2	1	0	7
M7	0	0	3	2	4	0	1	0	0	0
M8	0	0	3	3	0	0	0	0	0	0
M9	0	0	1	1	0	0	0	0	0	0
M10	0	0	0	0	0	0	0	0	0	0

Step 5. Use the worst occurrences data between the two different wind angles *(0^0 and 45^0)* for the data analysis as shown in Table 4.

Use the worst occurrence data between two wind angles under the same Range (R) and Mean (M) as per example below,

For *Table 2- M1R3 =* ***57*** occurrences while *Table-3 –M1R3 =* ***1*** occurrence

For further data analysis **57** number of occurrence for M1R3 is selected as shown in Table 4.